Direct Feature Extraction on Range Image Data

[a]Sonya Coleman, [b]Bryan Scotney and [a]Dermot Kerr
[a]School of Computing and Intelligent Systems, University of Ulster, Northland Road, Londonderry, Northern Ireland
[b]School of Computing and Information Engineering, University of Ulster, Cromore Road, Coleraine, Northern Ireland

Abstract
The requirement for scalable operators in image processing has emerged in recent years as research in the field of computer vision has shown that, typically, a feature in an image may exist significantly over a specific range of scales, with the detected strength of a feature depending on the scale at which the appropriate feature detection operator is applied. Recent research in computer vision has focussed on the use of range images to provide an almost 3-dimensional description of a scene. Feature-driven segmentation of range images has been primarily used for 3D object recognition, and hence the accuracy of the detected features has become a prominent issue. Feature extraction on range images has proven to be a more complex problem than on intensity images due to both the irregular distribution of range image data and the nature of the features that are present in range images. This paper presents a design procedure for scalable second order derivative operators that can be used directly on irregularly distributed and sparse data through the use of the finite element framework; such operator are hence appropriate for direct use on range image data without the requirement of data pre-processing.

1. Introduction

In recent years computer vision applications have increasingly begun to use range image data instead of, or in conjunction with, intensity image data [7]. This is largely because range imagery can be used to obtain reliable descriptions of 3-D scenes; a range image contains distance measurements from a selected reference point or plane to surface points of objects within a scene [3], allowing more information about the scenes to be recovered [2]. However, a range image contains information about only the visible surfaces of the objects, and not their hidden surfaces, and hence is often referred to as $2\frac{1}{2}$-D information [3].

One problem with range images is the extensive amount of data that is required to be stored for each individual image. This large volume of data makes direct interpretation of range images costly. To reduce the computation involved in interpreting range images, range image feature extraction and segmentation have been identified as means of scene representation and are used in applications such as object recognition [9, 14], motion analysis [16], and automated visual inspection [15]. Such segmentation techniques for range images can be generalised into two categories: region-based segmentation, where pixels are classified into regions, and edge-based segmentation, where the region boundaries are detected. Edge-based techniques are more reliable, as region-based techniques can tend to create distortion of region boundaries, can result in over-segmentation and results may depend on the initial region selection, even when applied to very simple segmentation tasks [12]. Among the research that has focussed on segmentation of range image data, there are four well-known algorithms developed in the University of South Florida [11], Washington State University [8], the University of Bern [13] and the University of Edinburgh [21]. The algorithm of [10] computes a planar fit for every pixel and then grows regions for those that have similar plane equations. The algorithm from Washington State University, which was originally developed for quadric surfaces and then modified by [8] to accept only first order surface fits, often results in oversegmented images. Jiang et al., [13] use the scan line approximation with region growing performed using a set of line segments rather than individual pixels. This algorithm is fast but does not preserve the object edges completely. Finally, [21] proposed an algorithm similar to that of [10]. Although it provides a good standard of segmentation, the

method is quite slow and is sensitive to noise. This paper presents feature detection methods that do not require uniform data distribution, preserving the edge localisation and hence addressing problems such as over- and under-segmentation found in the segmentation algorithms.

Whilst much research has been carried out to develop edge detection methods for range image data, little has focussed on the area of multiscale, or adaptive, edge detection methods. When features in an image that occur over a range of scales are extracted at only one scale, localisation error or false edges may be introduced. In order to successfully extract the various edge types found in range images, multiscale feature extraction algorithms are particularly pertinent for obtaining good feature localisation and reliability as smooth crease edges are low-frequency events and jump edges are high-frequency events.

Due to the locational irregularity of range image data, multiscale feature detection on range images is a significantly different problem than that on intensity images. In recent work, Coleman et al., have focussed attention on the design and implementation of scalable and adaptive first and second order derivative operators through the use of a finite element (FE) framework; such operators have been proven to perform successfully when compared with well-known intensity image feature detection operators [4, 17]. Taking advantage of the flexibility offered by the finite element method, these operators can be altered to remove the requirement for regularly located image data [5] and thus can prove to be successful for the purpose of feature extraction on range images. The framework has also been used to design and implement novel near-circular first and second order derivative operators [6, 18] that have been shown to improve edge orientation angular error. Such operators can play a key role in feature extraction for recognition, as accurate localisation of object edges is imperative.

This paper presents a brief overview of the range image representation and the design procedure for the scalable operators that we propose for use directly on the range data. Some preliminary results using second order derivative operators are presented and an overview of future work that will be carried out on the problem of directly processing range data, without any pre-processing requirements, is described.

2. Range Image Representation

We consider an irregularly sampled image to be represented by a spatially irregular sample of values of a continuous function *u(x,y)* of distance on a domain Ω. Our operator design procedure is then based on the use of a mesh generated using Delaunay triangulation. With each node *i* in the mesh is associated a piecewise linear basis function $\phi_i(x, y)$ which has the properties

$$\phi_i(x_j, y_j) = \begin{cases} 1 & \text{if } i = j \\ 0 & \text{if } i \neq j \end{cases}$$

where (x_j, y_j) are the co-ordinates of the nodal point *j* in the mesh. Thus $\phi_i(x, y)$ is a "tent-shaped" function with support restricted to a small neighbourhood centred on node *i* consisting of only those triangles that have node *i* as a vertex; ϕ_i is linear on each mesh triangle. We then approximately represent the image function *u* by a function $U(x, y) = \sum_{j=1}^{N} U_j \phi_j(x, y)$ in which the parameters $\{U_1, ..., U_N\}$ are mapped from the image intensity values at the *N* irregularly located nodal, or scatter, points. The approximate image function representation is therefore piecewise linear on each triangle and has value U_j at node *j*.

3. Weak Forms of Operators

We formulate image operators that correspond to weak forms of operators in the finite element method [1, 17, 18]. Operators used for smoothing may be based simply on a weak form of the image function, for which it is assumed that the image function $u(x, y)$ belongs to the Hilbert space $H^0(\Omega)$; that is, the integral $\int_\Omega u^2 d\Omega$ is finite. Feature detection and enhancement operators are often based on first or second derivative approximations (or combinations of these, such as the rotation invariant operators used in [19, 20], for which it is necessary that the image function $u(x, y)$ is constrained to belong to the Hilbert space $H^1(\Omega)$; i.e. the integral $\int_\Omega (|\underline{\nabla} u|^2 + u^2) d\Omega$ is finite, where $\underline{\nabla} u$ is the vector $(\partial u/\partial x, \partial u/\partial y)^T$.

Corresponding to a second directional derivative $-\underline{\nabla} \cdot (\mathrm{B}\underline{\nabla} u)$, we may use a test function $v \in H^1(\Omega)$ to define the weak form

$$Z(u) = -\int_\Omega \underline{\nabla} \cdot (\mathrm{B}\underline{\nabla} u) v d\Omega .$$

Here $\mathbf{B} = \underline{b}\ \underline{b}^{\mathrm{T}}$ and $\underline{b} = (\cos\theta, \sin\theta)$ is the unit direction vector. Zero-crossing methods are often based on the isotropic form of the second order derivative, namely the Laplacian $-\underline{\nabla}.(\underline{\nabla} u)$. This is equivalent to the general form in which the matrix **B** is the identity matrix **I**.

In the finite element method a finite-dimensional subspace $S^h \subset H^1$ is used for function approximation; in our design procedure the irregular image U is a function in S^h, and S^h is defined by the irregular mesh of triangular elements and piecewise linear basis functions described in Section 2.

Since we are focusing on the development of operators that can explicitly embrace the concept of size and shape, our design procedure uses a finite-dimensional test space $T_\sigma^h \subset H^1$ that explicitly embodies a size parameter σ that is determined by the local scatter point density. This generalisation allows sets of test functions $\psi_i^\sigma(x, y)$, i=1,…,N, to be used when defining irregular derivative based operators; for second order operators, this provides the functional

$$Z_i^\sigma(U) = \int_\Omega \underline{\nabla} U \cdot (\mathrm{B}_i \underline{\nabla} \psi_i^\sigma) d\Omega .$$

4. Direct Processing Algorithm

The test space T_σ^h comprises a set of Gaussian basis functions $\psi_i^\sigma(x, y)$, i=1,…,N of the form

$$\psi_i^\sigma(x, y) = \frac{1}{2\pi\sigma^2} e^{-\left(\frac{(x-x_i)^2 + (y-y_i)^2}{2\sigma^2}\right)} .$$

Each test function $\psi_i^\sigma(x, y)$ is restricted to have support over a neighbourhood Ω_i^σ, centred on node i, consisting of those triangular elements that have node i as a vertex. We note therefore that the integrals in the definitions of the functional Z_i^σ can be computed by integration over only the neighbourhood Ω_i^σ rather than the entire image domain Ω, providing the functional

$$Z_i^{\sigma}(U) = \int_{\Omega_i^{\sigma}} \underline{\nabla} U \cdot (\mathrm{B}_i \underline{\nabla} \psi_i^{\sigma}) d\Omega_i \cdot$$

4.1 Local Size Selection

The usually difficult issue of local size selection for an operator is now naturally addressed by the distribution of the nodes in the mesh-based representation of the image. For a scatter point (x_i, y_i) we obtain the local operator size directly from the mesh in the neighbourhood Ω_i^{σ}. We consider an approach which we have named the *Primrose* algorithm.

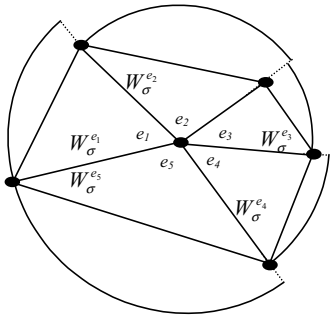

***Primrose* Operator**

Figure 1. Neighbourhoods Ω_i^{σ} in irregular mesh.

In the *Primrose* algorithm the neighbourhood Ω_i^{σ} is defined to have a real-valued "radius" $W_{\sigma}^{e_m}$ for each element e_m in Ω_i^{σ}. In each case $W_{\sigma}^{e_m}$ is chosen as the radius of the smallest circle centred on (x_i , y_i) containing element e_m. Each element therefore contributes a "petal" to the *Primrose* operator as illustrated in Figure 1. The test function ψ_i^{σ} is correspondingly comprised of a set of sectors of Gaussian functions $\psi_i^{\sigma_m}$, where $\psi_i^{\sigma_m}$ is the test function over element e_m in Ω_i^{σ}. In each case choosing the element scale parameter $\sigma_m = W_{\sigma}^{e_m} / 1.96$ ensures that along the longest element edge of e_m through (x_i, y_i) 95% of the cross-section of the Gaussian is contained in e_m.

Construction of these operators on an irregular grid differs significantly from construction of image processing operators on a regular grid in that it is no longer appropriate to build explicitly an entire operator as in [17]; each operator throughout an irregular mesh may be different with respect to the operator neighbourhood size, shape, and the number of nodal points in the operator. When using an irregular grid, we work on an element-by-element basis to build each operator, taking advantage of the flexibility offered by the finite element method as a means of adaptively changing the irregular operator size and shape to encompass the data available in any local neighbourhood. Such local neighbourhoods are illustrated by the collections of triangular elements shown in Figure 2; in each neighbourhood the test function ψ_i^{σ} is comprised of a set of sectors of Gaussian functions $\psi_i^{\sigma_m}$ truncated at "radius" $W_{\sigma}^{e_m}$. Thus each operator is able to automatically alter its shape and size as required, dependent on the irregular node placement corresponding to the sampling of the image data. Operator *a* in Figure 2 has a central node with 5 adjoining nodes, operator *b* illustrates 7 adjoining nodes and operator *c* illustrates 6 adjoining nodes.

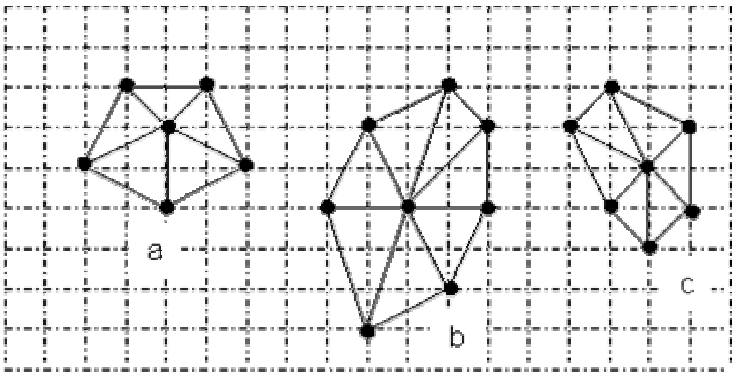

Figure 2. Neighbourhoods of Operators

4.2 Efficient Implementation

The spatial relationship between the node i on which the Gaussian basis function ψ_i^σ is centred and each of the nodes in the neighbourhood Ω_i^σ is readily available from nodal numbering and locational information routinely stored in the finite element method. The integrals required in the computation of operators such as $Z_i^\sigma(U)$ are evaluated through the standard process of finite element assembly: integrals $k_{is}^{m,\sigma}$ over each element $e_m \subset \Omega_i^\sigma$ are approximately evaluated using Gaussian quadrature rules, requiring function evaluations in e_m of the test function ψ_i^σ and of the three piecewise linear basis functions ϕ_s (locally indexed s = 1,2,3) whose support includes element e_m. Since the first derivatives of the piecewise linear basis functions are locally constant, each element integral may be accurately approximated by just four function evaluations (i.e., using a four-point Gauss rule). The issue of evaluating integrals over irregularly shaped triangular elements is routinely handled in the finite element method by the use of isoparametric mappings that relate each element to a "standard" right-angled triangle on which numerical integration can be efficiently and accurately performed [1].

5. Results

To illustrate results for our proposed technique, we use 256×256 range images taken from the Ohio State University range image database [22]. In order to apply our technique directly to the irregular range image data, we initially use Delaunay triangulation to generate a triangular mesh in which the irregular image data points are nodes. As the nodal point set simply corresponds to the co-ordinates of the irregular image data, the local density of nodes in this mesh is simply controlled by the local availability of data points. This mesh is then used as the basis for the application of the finite element based operators described in Sections 3 and 4. Figure 3 illustrates the original 256×256 range images and the corresponding feature images generated using Marr-Hildreth's Laplacian of Gaussian operators of size 5×5 (MH5) and 7×7 (MH7) and the proposed technique. The results presented are preliminary, as the work is at an exploratory stage of development. In [4, 5, 6, 17, 18] both first and second derivative operators are designed and used for feature extraction from irregular data. First and second derivative operators can be combined to yield rotation invariant operators of the form used in [19, 20], and our preliminary evaluation will be extended to embrace such combinations. A systematic evaluation based on comparative results with the methods in [8, 11, 13, 21] is in preparation.

(a) Original Range Image

(b) MH5 $T = 1$

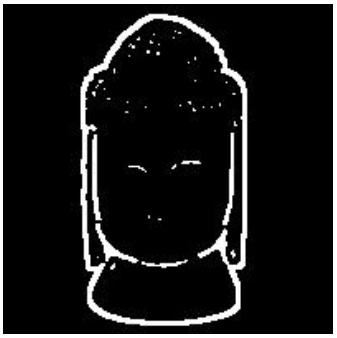

(b) MH7 $T = 1$

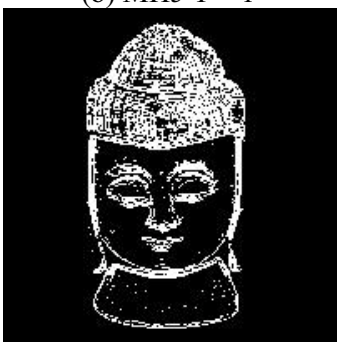

(c) *Primrose* $T = 22$

Figure 3. Feature maps generated using the Marr-hildreth Operators and the Primrose algorithm

(a) Original Range Image

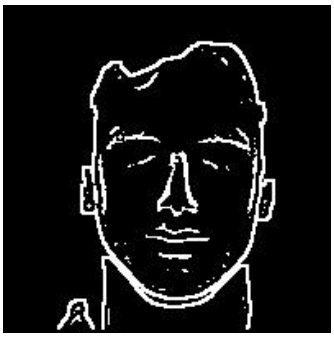

(b) MH5 $T = 1$

(c) MH7 $T = 1$

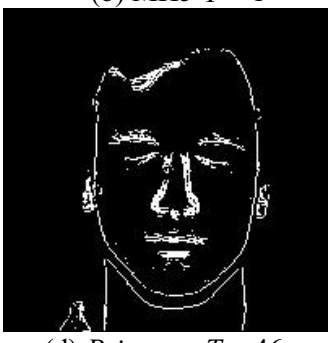

(d) *Primrose* $T = 46$

Figure 4. Feature maps generated using the Marr-hildreth Operators and the Primrose algorithm

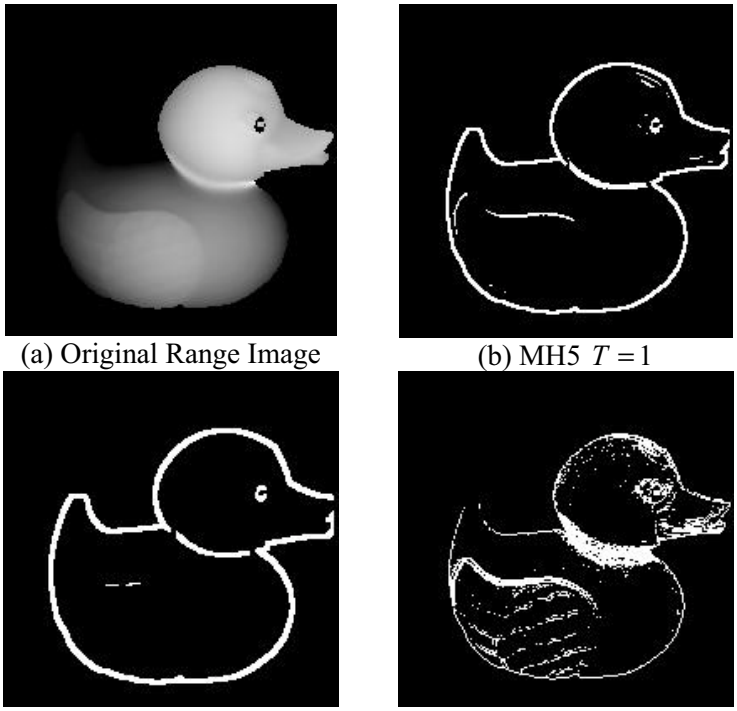

(a) Original Range Image (b) MH5 $T = 1$

(c) MH7 $T = 1$ (d) *Primrose* $T = 6$

Figure 5. Feature maps generated using the Marr-hildreth Operators and the Primrose algorithm

In order for the Marr-Hildreth operators to be applied to the range images, the range image data was projected onto a regular mesh using the `griddata` function in Matlab. Figures 3, 4, and 5 illustrate that the second order *Primrose* algorithm detected finer edges and more features than the Marr-Hildreth algorithm and as the *Primrose* algorithm can be applied directly to the range data, the features detected in Figures 3(d), 4(d) and 5(d) should be more accurately located than those detected by the Marr-Hildreth algorithm.

6. Summary and Future Work

The overall aim of this research is to develop and implement multiscale feature extraction algorithms for direct use on irregular or incomplete range image data, improving feature localisation and enabling real-time processing for the application of robotic vision. Current results as presented in the paper in the form of second order feature maps are promising and such techniques need to be refined and timed in order to prove their worth. The feature maps presented here are compared with those generated using the Marr-Hildreth technique. Whilst the Marr-Hildreth operators are not entirely appropriate for use on range images, they do provide some preliminary comparative results. Future work will initially involve generating irregular quadrilateral operators using bilinear basis functions in order to reduce the processing time towards achieving real-time computation as an image sequence is captured. Such operators will then be adapted in order to determine the nature of the features detected: crease, jump or smooth. Such techniques will be used for segmentation and will be evaluated with respect to existing edge based segmentation algorithms, with the overall goal of recognising objects in range image sequences in real-time.

7. References

[1] Becker, E.B., Carey, G.F., and Oden, J.T., *Finite Elements: An Introduction*, Prentice Hall, London, 1981.

[2] Bellon, O., and Silva, L., "New Improvements on Range Image Segmentation by Edge Detection Techniques" *Proceedings of the workshop on Artificial Intelligence and Computer Vision,* Nov. 2000.
[3] Besl, P.J., "Active, optical range imaging sensors."*Machine Vision and Apps*, Vol.1, pp127-152, 1988.
[4] Coleman, S.A., Scotney, B.W. & Herron, M.G.., "Adaptive Edge Detection using Image Variance." *Proc. of 6th Irish Machine Vision and Image Processing Conference (IMVIP2002).*
[5] Coleman, S.A., Scotney, B.W. & Herron, M.G. "Image Feature Detection on Content-Based Meshes *Proc. of IEEE Int. Conf on Image Processing (ICIP2002),* pp. 844-847
[6] Coleman, S.A., Scotney, B.W. & Herron, M.G.., "A Systematic Design Procedure for Scalable Near-Circular Laplacian of Gaussian Operators." *Proc. ICPR* 2004.
[7] Dias, P., et al., "Combining Intensity and Range Images for 3D Modelling", *Proc. IEEE International Conference on Image Processing (ICIP2003)*.
[8] Flynn, P.J., and Jain, A.K., "BONSAI: 3D Object Recognition Using Constrained Search" *IEEE Trans. Pattern Analysis and Machine Intelligence*, Vol 13, No. 10, pp.1066-1075, 1991.
[9] Flynn, P.J., and Jain, A.K., "Three-dimensional object recognition" *Handbook of Pattern Recognition and Image Processing: Computer Vision*, Academic Press, San Diego, pp 497-541, 1994.
[10] Goldgof, D.B., et al., "A Curvature-Based Approach to Terrain Recognition" *IEEE Trans. Pattern Analysis and Machine Intelligence*, Vol 11, pp.1213-1217, 1989.
[11] Gunsel, B., et al., "Reconstruction and boundary detection of range and intensity images using multiscale MRF representations" *CVIU*, Vol. 63, pp353-366, 1996.
[12] Hoover, A. et al., "An Experimental Comparison of Range Image Segmentation Algorithms" *IEEE Trans. Pattern Analysis and Machine Intelligence,* Vol 18, No. 7, pp.673-689, 1996.
[13] Jiang, X. Y., and Bunke, H., "Fast Segmentation of Range Images into Planar Regions by Scan Line Grouping", *Machine Vision and Applications*, Vol. 7, No. 2, pp115-122, 1994.
[14] Kaveti, S., et al., "Second-Order Implicit Polynomials for segmentation of Range Images." *Pattern Recognition*, Vol. 29, No. 6, pp. 937-949, 1996.
[15] Newman, T.S., and Jain, A.K., "A system for 3D CAD-based inspection using range images" *Pattern Recognition*, Vol. 28, No. 10, pp 1555-1574, 1995.
[16] Sabata, B., and Aggarwal, J.K., "Surface correspondence and motion computation from a pair of range images", *Computer Vision and Image Understanding*, Vol. 63, pp 232-250, 1996.
[17] Scotney, B.W. et al., "Device Space Design for Efficient Scale-Space Edge Detection." *Proc Int. Conf. on Computational Science (ICCS2002).* Springer-Verlag, LNCS.
[18] Scotney, B.W. et al., "Improving Angular Error by Near Circular Operator Design" *Pattern Recognition, Elsevier* Vol. 37(1), pp169-172, 2004.
[19] Schiele, B. and Crowley, J.L. "Object Recognition using Multidimensional Receptive Field Histograms", *Proc. 4th European Conference on Computer Vision*, 1996, pp. 610-619.
[20] Schmid, C. and Mohr, R., "Combining Grayvalue Invariants with Local Constraints for Object Recognition", *Proc. International Conference on Computer Vision and Pattern Recognition*, 1996, pp. 872-877.
[21] Trucco, E., and Fisher, R.B., Experiments in Curvature-Based Segmentation of Range Data", *IEEE Trans. Pattern Analysis and Machine Intelligence,* Vol 17, No. 2, pp. 177-182, 1995.
[22] http://sampl.eng.ohio-state.edu/~sampl/data/3DDB/RID/index.htm